

Two-dimensional spin-1 frustrated Heisenberg model with valence-bond ground states

Zi Cai¹, Shu Chen^{1,*}, Supeng Kou², and Yupeng Wang¹

¹*Beijing National Laboratory for Condensed Matter Physics, Institute of Physics, Chinese Academy of Sciences, Beijing 100080, P. R. China*

²*Department of physics, Beijing Normal University, Beijing 100875, P. R. China*

(Dated: Received February 4, 2008)

In this paper, we propose a method to understand the nature for the quantum disorder phase of the two-dimensional (2D) high spin frustrated model. The ground state and excitation properties of a fully frustrated 2D spin-1 model are studied based on a model whose groundstate can be found exactly. By analogy to the pseudo-potential approach in the fractional quantum Hall effect, we conclude that the ground states of the fully frustrated spin-1 model are doubly degenerate valance bond solid (VBS) states along the horizontal or vertical direction of the square lattice. We also find that the ground state could be characterized by a nonzero string order, which rarely happened in the 2D case. The method that we used reveals the connection between the fractional quantum hall effect and the frustrated 2D antiferromagnetism system. The VBS states capture the main character of the disordered phase in the 2D spin-1 frustrated system, and can be verified by a numerical method.

PACS numbers: 75.10.Jm, 71.27.+a, 75.10.-b

I. INTRODUCTION

The 2D quantum frustrated magnets have attracted considerable attention in the past years¹ because they are believed to be promising candidates for realizing exotic spin liquid states. One of the most studied 2D frustrated models is the antiferromagnetic Heisenberg model on a square lattice with the first and second nearest neighbor interactions J_1 and J_2 ,

$$H = J_1 \sum_{\langle i,j \rangle} \mathbf{S}_i \cdot \mathbf{S}_j + J_2 \sum_{\langle\langle i,j \rangle\rangle} \mathbf{S}_i \cdot \mathbf{S}_j \quad (1)$$

where $\langle i,j \rangle$ and $\langle\langle i,j \rangle\rangle$ represent pairs of the nearest and next-nearest neighbors respectively. The general ground state properties of this model have been investigated in various methods^{2,3,4,5,6}. It has been well accepted that the $J_1 - J_2$ model exhibits a quantum phase transition from a magnetically ordered Néel phase at small J_2/J_1 to a spin disordered phase in the intermediate parameter region. Despite the success in predicting the order to disorder transition, the theory based on mapping onto the non-linear σ model and symmetry analysis provides no clear information about the nature of the disordered phase. For the 2D spin-1/2 $J_1 - J_2$ model, there have been a lot of works focusing on its nonmagnetic phase, but no definite conclusion has been drawn on the controversial question whether the disordered phase is a spin liquid without symmetry breaking or a valence bond crystal with broken spatial symmetry^{7,8}.

Most researches in this field focus on the spin-1/2 system because of its possible correlation with the High-Tc superconductivity. However, in recent years ultracold atomic system has provided an ideal playground to experimentally investigate the high-spin strongly correlated system. Several proposals have been provided to realize the spin-1 lattice model⁹. Considering the rapid development in this field, we expect that it is possible for the spin-1 $J_1 - J_2$ model to be realized experimentally in

the future. However, in comparison with the spin-1/2 system, little knowledge is known about the disordered phase of the 2D spin-1 system except the possible double degeneracy of the ground state predicted by the field theory⁶.

In this paper we first review some general results of the disordered phase in the frustrated model, then we investigate the ground state properties of a fully frustrated spin-1 $J_1 - J_2$ model with $J_2/J_1 = 0.5$ by the pseudo-potential approach. Our method can be generalized to deal with other systems such as the frustrated honeycomb model and system with higher spin.

The general property for the 2D spin 1 frustrated model was investigated in the scope of the (2+1)-dimensional nonlinear σ model^{3,4}, which is considered as the continuum limit of the SU(N) antiferromagnet^{6,10}. Though this model was derived in the semiclassical (large S) limit and no frustrated condition, it is still valid to describe the condition of small S and frustrated case^{3,4}. The effective action of a 2D spin-1 $J_1 - J_2$ model is

$$S_{\text{eff}} = \frac{1}{2g_0} \int d\tau d^2\mathbf{r} \left\{ \frac{1}{c} (\partial_\tau \mathbf{m})^2 + c (\nabla \mathbf{m})^2 \right\} + S_B \quad (2)$$

where $S_B = iS \sum_{\mathbf{R}} \eta_{\mathbf{R}} \oint d\mathbf{m}_{\mathbf{R}} \cdot \mathbf{A}_{\mathbf{R}}$, $g_0 = \frac{\sqrt{8a}}{S\sqrt{1-2\alpha}}$ and $c = \sqrt{8(1-2\alpha)}J_1Sa$ with $\alpha = J_2/J_1$. This is precisely the O(3) non-linear σ model in the (2+1) dimensions with a residual Berry phase (S_B). Via this model, renormalization group (RG) analysis predicted that there is a transition from the Néel state to a disordered state and the transition point for the spin-1 model is $\alpha_c = 0.46$, larger than that in spin-1/2 case. The Berry phase plays a crucial role in determining the degeneracy and symmetry of the ground state in the disordered phase^{6,10}. For the spin-1 model, the degeneracy in the disordered phase is 2 and there is a spontaneous symmetry breaking. We will see below that the symmetry of our trial ground states completely agrees with that predicted by the general theory above.

The analogy between the Heisenberg model and the fractional quantum Hall effect (FQHE) was first introduced by Arovas *et al.*¹¹ in the one-dimensional (1D) case. They decomposed the spin-1 antiferromagnetic Heisenberg Hamiltonian as:

$$H_1 = \sum_i \mathbf{S}_i \cdot \mathbf{S}_{i+1} = \sum_i [3P^2(i, i+1) + P^1(i, i+1) - 2] \quad (3)$$

while they treat the projection operator $P^1(i, i+1)$ over spin-1 states associated with two consecutive sites as a perturbation and consider the Affleck-Kennedy-Lieb-Tasaki (AKLT) state¹², which is the exact ground state of the projection operator $3P^2(i, i+1)$ over spin-2 states, as a trial ground state of the spin-1 Heisenberg chain. The AKLT state and the real ground state of the spin-1 Heisenberg chain share a lot of important properties, for example both of them have an energy gap and the two point correlation functions decay exponentially. They are in the same universal class and characterized by a hidden order parameter called “string parameter”.¹³ Numerical results show that the difference between the ground state energies of these two states is within 5%. In this work, we extended their method to the 2D fully frustrated model to study the properties of the groundstate and the elementary excitation.

For the fully frustrated model with $J_2/J_1 = 0.5$, we can rewrite the Hamiltonian Eq.(1) as:

$$H = \sum_{\alpha} H_{\alpha} \quad \text{with} \quad H_{\alpha} = J_2 \sum_{i,j \in \alpha} \mathbf{S}_i \cdot \mathbf{S}_j, \quad (4)$$

where the index α denotes the site of the dual lattice corresponding to the α th plaquette. Each bond interaction between the two spins in a plaquette is equal. For convenience, we expand this Hamiltonian by the projection operators of total spin in a plaquette:

$$H_{\alpha}/J_2 = \sum_{S=0}^4 C_S \mathbf{P}_{\alpha}^S - 4 \quad (5)$$

with $C_s = S(S+1)/2$ and further decompose it as the summation of two parts:

$$H_{\alpha} = H_{\alpha}^0 + H_{\alpha}^1,$$

with

$$\begin{aligned} H_{\alpha}^0/J_2 &= 10\mathbf{P}_{\alpha}^4 + 6\mathbf{P}_{\alpha}^3 - 4, \\ H_{\alpha}^1/J_2 &= 3\mathbf{P}_{\alpha}^2 + \mathbf{P}_{\alpha}^1. \end{aligned}$$

The operator \mathbf{P}_{α}^S projects the spin state of the α th plaquette onto the subspace with total spin S . One of the reasons for dividing the original Hamiltonian into two parts is that the model $H^0 = \sum_{\alpha} H_{\alpha}^0$ is quasi-exactly solvable in the sense that its ground state can be obtained exactly. Furthermore, we observe that the coefficient C_S decreases rapidly as S descends. Therefore it is reasonable to apply the pseudo-potential method originally used

in the FQHE¹⁴. Using this method, we first classify all the ground states of H^0 and treat $H^1 = \sum_{\alpha} H_{\alpha}^1$ as a perturbation. The ground state of H^0 is shown to be highly degenerate and belongs to two kinds of states: the dimer states and the valence bond solid states. However the huge degeneracy of the ground states is lifted when H^1 is introduced. Finally our result shows that the ground states of the fully frustrated spin-1 model are doubly degenerate and approximately described by the decoupled VBS states along the horizontal or vertical direction of the square lattice. We believe that our work would inspire the interest in the spin-1 frustrated model.

II. THE SPIN-1 MODEL WITH EXACT GROUND STATES

Now we start by considering a spin-1 Hamiltonian on a square lattice:

$$H_p = \sum_{\alpha} (c_4 \mathbf{P}_{\alpha}^4 + c_3 \mathbf{P}_{\alpha}^3), \quad (6)$$

where H_p is an arbitrary linear composition of projection operators \mathbf{P}_{α}^4 and \mathbf{P}_{α}^3 with $c_4, c_3 \geq 0$. Obviously, H^0 is just a special case of the above Hamiltonian. Since H_p is positive semidefinite, the state with the total spin of each plaquette $S_{\alpha}^T \leq 2$ is the exact ground states for H_p . Such a condition could be satisfied by two kinds of states: *the dimer states* and *the valence bond solid states*.

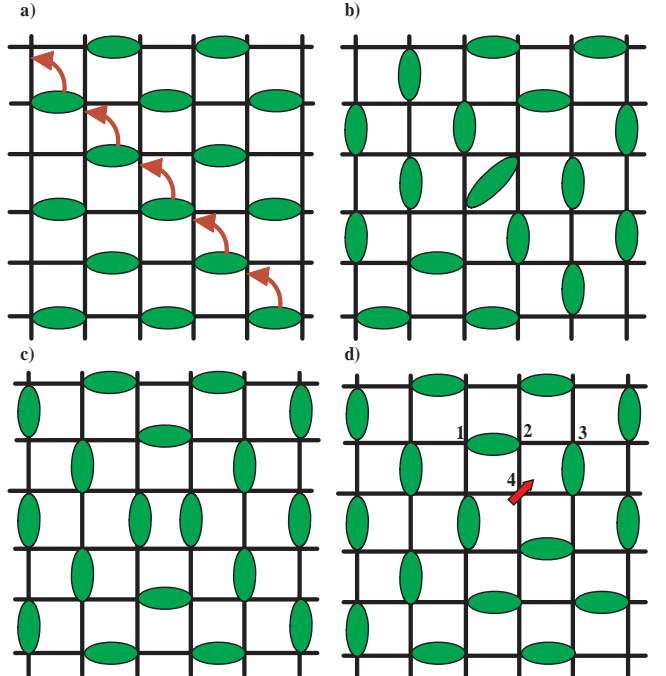


FIG. 1: (Color online) Different dimer ground states of H_p . The green (dark) ellipsoids represent singlet dimers formed by two $S = 1$ spins.

The dimer states are the states with each plaquette possessing a dimer, which is a spin singlet formed by two neighboring spins: $\frac{1}{\sqrt{3}}(|1, -1\rangle + | - 1, 1\rangle - |00\rangle)$. This family of states are illustrated in Fig.1 and are very similar to the dimer ground states in the spin-1/2 case¹⁵ except the singlet dimers are formed by pairs of spin with $S = 1$ and also the defect spin in Fig. 1(d) has $S = 1$. As stated by Batista *et al.*, the states in Fig.1 (a-d) represent all the possible configurations which satisfy the constrain that every plaquette possesses at least one dimer¹⁵. For the configuration in Fig.1(a), rotating any array of dimers along a diagonal direction by $\pi/2$, we will get a new degenerate state of this model, as stated in¹⁵. The degeneracy of this kind of ground state is proportional to $2^{\sqrt{N}+1}$, where N is the total number of the sites. States in Fig.1(b-d) represent the configurations with one "defect" and it is possible to have a localized $S = 1$ spin as illustrated in Fig. 1(d). Translating or rotating these kinds of states around the central defect gives a huge amount of degeneracy proportional to N , the total number of the sites. Configurations in Fig. 1(a-d) and their corresponding degeneracy states provide a full configuration subspaces that satisfy the constraint that each plaquette has at least one singlet.

For the spin-1 system, however, there may be another family of ground state totally different from that of the spin-1/2 case: the VBS state, or the AKLT state¹². An $S = 1$ spin in one site could be considered as a symmetric composition of two $S = 1/2$ spins and the AKLT state is formed by the valence bond, which is the singlet state of two neighboring $S = 1/2$ spins. If there is a global state ensuring that each plaquette has at least two valence bonds, as illustrated in Fig.2(a-f), such a state is also a ground state of H_p due to $S_\alpha^T \leq 2$. Obviously, this kind of ground state is also highly degenerate. The lattice we considered is under the open boundary condition with the total site of lattice $N \rightarrow \infty$. Configurations in Fig.2(a-c) are composed by many 1D AKLT chains with infinite length. Fig.2(d-e) represent the configurations composed by the closed AKLT loop and a defect in the center. Other configurations not listed here which satisfy the same constraint are similar to Fig.2(e,f), but with a defect of a different shape. We could estimate that the number of this kind of degeneracy is proportional to N by considering the possible positions of the central defect in Fig.2(d-f).

Now we focus on the excitation of the second family. The elementary excitation of the AKLT chain is the magnon excitation with a Haldane gap of 0.35¹¹, in which a singlet dimer formed by two neighboring $S = 1/2$ spins is excited to a triplet state, as illustrated in Fig.3(a). Unlike the dimer case, these two 1/2 spinons could not be separated without increasing the energy proportional to the distance between them, so this kind of excitation is confined. However, the triplet state itself, which is formed by two binding spinons, could propagate along the AKLT chain freely, as shown in Fig.3(b).

It is noted that a similar method has been used to con-

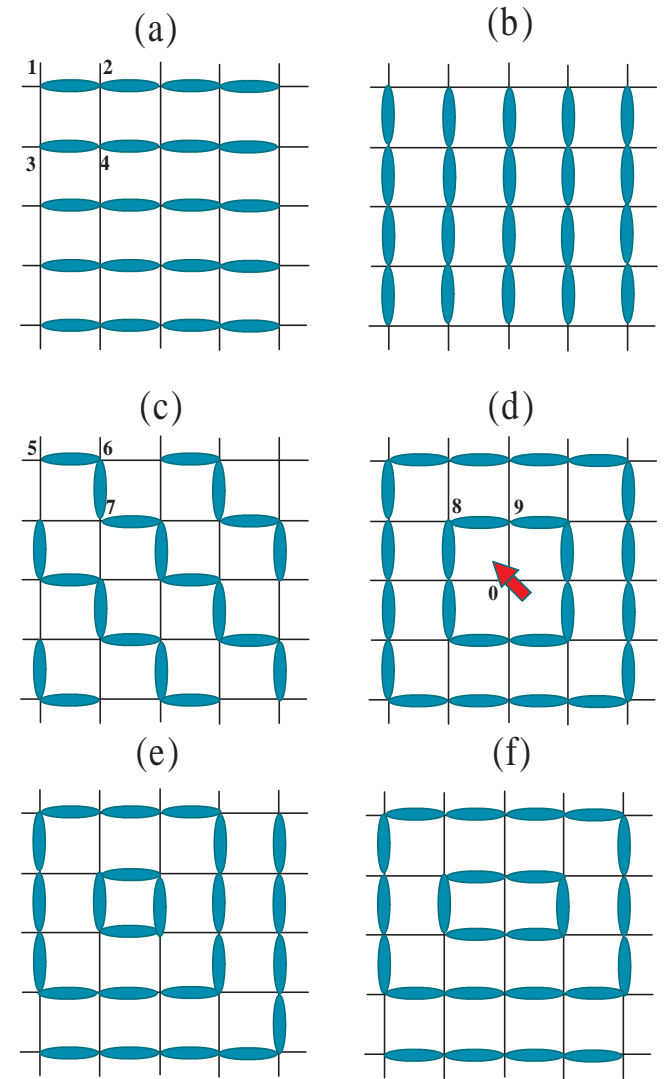


FIG. 2: (Color online) Different AKLT ground states of H_p . The blue (dark) ellipsoids represent singlet states formed by two $S = 1/2$ pseudospins.

struct the exact ground state of the well known 1D AKLT model¹² and the 2D spin-1/2 model with additional cyclic exchanges¹⁵. The application of such a method has made a lot of success in understanding the nature for spin systems^{12,15,16,17,18}.

III. THE GROUND STATE OF THE $J_1 - J_2$ MODEL WITH FULL FRUSTRATION

Since the Hamiltonian Eq.(6) is somehow an artificial model, how could we expect that it is related to the fully frustrated $J_1 - J_2$ model? We will clarify this problem below using the analogy to the pseudopotential approach in the FQHE¹⁴, where, restricted within the first Landau level, the interaction can be expanded by relative

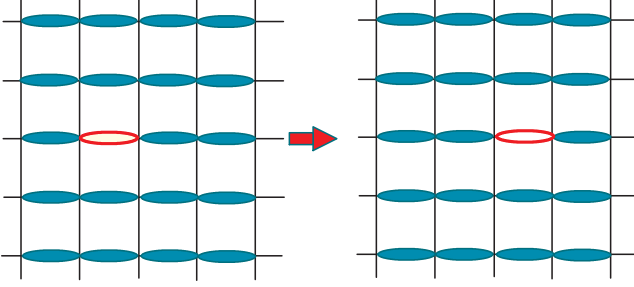


FIG. 3: (Color online) (a) One singlet is excited to a triplet (open ellipsoid). (b) The excitation could propagate along the AKLT chain freely. The blue (dark) ellipsoids represent singlets formed by two pseudospins with $S = 1/2$.

angular momentum projection operators: $v(r_i - r_j) = \sum_{k=0}^{\infty} v_k P_k(ij)$ with $P_k(ij)$ the projection operator on states with angular momentum k . If a potential satisfies $v_k=0$ when $k \geq m$, the Laughlin state is the exact ground state for this model. The success of this method depends on the difference between the coefficient v_k of $k = m - 2$ and $k = m^{14}$.

Now we treat the 2D $J_1 - J_2$ Hamiltonian in the spirit of the pseudopotential approach and consider H_{α}^1 as perturbation of H_{α}^0 , just as Arovas et. al did in the 1D case. Since the ground state of $H^0 = \sum_{\alpha} H_{\alpha}^0$ has been analyzed above, all the degenerate ground states of Hamiltonian (6) may be a possible candidate of the trial ground state for the Hamiltonian (4). However, the perturbation $H^1 = \sum_{\alpha} H_{\alpha}^1$ lifts the high degeneracy and chooses some states as the best trial ground state.

Next we will calculate the energy expectation under those degenerate states. The lower the expectation value is, the closer the state is to the real ground state of (4). We notice that our lattice is constructed by the bonds connecting one site with its nearest neighborhood or the next nearest ones. To calculate the average energy of various candidate trial groundstates, we must first calculate the energy expectation of each bond. For the dimer states as shown in Fig.1, all the configurations in Fig.1 (a-d) are constructed by three kinds of bonds. Take the Fig.1 (d) for an example: the first kind is represented by bond 12, which is covered by a single dimer. Bond 23 represents the bond between two different dimers, and the third kind (bond24) is the one between a dimer state and a single spin with $S = 1$. The energy expectations for these three kinds of bonds are

$$\begin{aligned} \langle \mathbf{S}_1 \cdot \mathbf{S}_2 \rangle_{\text{dimer}} &= -2, \\ \langle \mathbf{S}_2 \cdot \mathbf{S}_3 \rangle_{\text{dimer}} &= \langle \mathbf{S}_2 \cdot \mathbf{S}_4 \rangle_{\text{dimer}} = 0, \end{aligned} \quad (7)$$

respectively. It is ready to calculate the average energy per plaquette in the thermodynamic limit:

$$\langle E \rangle_{\text{dimer}} = -2J_2,$$

which is the same for all the configurations in the Fig.1 (a-d).

Now we turn to the VBS states in Fig.2. Similar to the method above, we can classify all the bonds which construct the configurations in Fig.2 into five classes: (1) Bond 12 or 34 in Fig.2(a), which is covered by a valence bond formed by the singlet of two $1/2$ spinons in a AKLT chain with infinite length; (2) Bond 57 in Fig.2(c) is the bond connecting two next nearest sites in an AKLT chain; (3) Bond 13 or 24 in Fig.2(a) which connects different AKLT chains; (4) Bond 89 in Fig.2(d) is similar to the first one, but the bond is covered by a valence bond in a closed AKLT loop with finite length; (5) Bond 90 in Fig.2(d) is the bond between one site in an AKLT chain and another site occupied by a single spin with $S = 1$.

Now we calculate the average energy under all these candidate trial ground states in Fig.2 to find which one has the lowest energy. We define $\mathbf{T}_{\pi/2}$ as an operator to rotate the system by $\pi/2$ around one site in the lattice. So we can see that $\Psi_{\text{AKLT}\parallel}^a = \mathbf{T}_{\pi/2} \Psi_{\text{AKLT}\parallel}^b$, and the Hamiltonian in Eq.(1) is invariant under the operator $\mathbf{T}_{\pi/2}$. So the states in Fig.2(a) and (b) are degenerate. We denote these states as $\Psi_{\text{AKLT}\parallel}$. In a similar way, we can get

$$\langle \mathbf{S}_1 \cdot \mathbf{S}_2 \rangle_{\text{AKLT}\parallel} = \langle \mathbf{S}_3 \cdot \mathbf{S}_4 \rangle_{\text{AKLT}\parallel} = -4/3$$

while other bonds all contribute zero to the average energy. It is clear that we have

$$\langle E \rangle_{\text{AKLT}\parallel} = -\frac{8}{3} J_2,$$

which is smaller than $\langle E \rangle_{\text{dimer}}$. If we consider the states like Fig.2(c), where there are many right angles along the AKLT chain, we find that the average energy under these states denoted by $\Psi_{\text{AKLT}\perp}$ is always higher than that of $\Psi_{\text{AKLT}\parallel}$. In the AKLT state, there is a short range correlation¹², and thus we get

$$\langle \mathbf{S}_5 \cdot \mathbf{S}_7 \rangle = 4/9,$$

whereas we have $\langle \mathbf{S}_5 \cdot \mathbf{S}_6 \rangle = \langle \mathbf{S}_6 \cdot \mathbf{S}_7 \rangle = -4/3$. So this kind of bonds in the corner of the AKLT chain would always raise the average energy of the system. We can find in Fig.2(d) $\langle \mathbf{S}_9 \cdot \mathbf{S}_9 \rangle = 0$ So the energy of configurations corresponding to Fig.2(d-f) and other configurations not listed here is always higher than the energy of $\Psi_{\text{AKLT}\parallel}^a$ and $\Psi_{\text{AKLT}\parallel}^b$ for two reasons: the appearance of right angles along an AKLT chain as well as the fact that the average value of $\mathbf{S}_i \cdot \mathbf{S}_{i+1}$ is lower in an AKLT chain with infinite length than that in a closed AKLT loop with finite length, *i.e.*, $\langle \mathbf{S}_1 \cdot \mathbf{S}_2 \rangle_{\text{AKLT}\parallel} < \langle \mathbf{S}_8 \cdot \mathbf{S}_9 \rangle_{\text{AKLT}\square}$. The proof of this fact has been shown in the Appendix.

As we showed above, the perturbation lifts the degeneracy and chooses state $\Psi_{\text{AKLT}\parallel}^a$ and $\Psi_{\text{AKLT}\parallel}^b$ (shown in Fig.2 (a, b)) as trial ground states. Apparently, they are doubly degenerate. It is natural to ask how close they are to the real ground states. Here we give an estimation. We can expand $\Psi_{\text{AKLT}\parallel}^a$ in the spirit of the pseudo-potential approach: $\Psi_{\text{AKLT}\parallel}^a = a\Psi_2 + b\Psi_1$, where

$\Psi_\beta = \sum_\alpha P_\alpha^\beta \Psi_{AKLT\parallel}^a$ ($\beta = 1, 2$) and $a^2 + b^2 = 1$. The reason why there is no component of Ψ_0 is that if there exists a state in which the total spin of every plaquette is zero, the energy for every plaquette gets to its minimum simultaneously which is impossible because the wave function would not be self-consistent. Observing that $\langle \mathbf{S}_{total}^2 \rangle_{AKLT\parallel} = 6a + 2b = 8/3$, we can get the coefficient $b = 0.994$, which means $\langle \Psi_{AKLT\parallel}^a | \Psi_1 \rangle = 0.994$. Based on this result, we can reconfirm the validity of the perturbation used above. Because Ψ_1 is the dominant part in $\Psi_{AKLT\parallel}^a$, the operator \mathbf{P}_α^1 in the perturbation H^1 plays a more important role than \mathbf{P}_α^2 . Furthermore since the coefficient of \mathbf{P}_α^1 is smaller than that of \mathbf{P}_α^2 , the effect of the perturbation to the unperturbed state is even smaller. Therefore, we believe that this trial state should be a good approximation to the ground state of Hamiltonian (4).

Nevertheless, it seems that there is still a question to be clarified. Since the trial ground states $\Psi_{AKLT\parallel}^a$ and $\Psi_{AKLT\parallel}^b$ are degenerate, we should use the degenerate perturbation rather than that used above, which means that a linear composition of these two degenerate states could further lower the energy and forms a new ground state, just as in the resonant valence bond theory. We shall show that it is not true in this case. As we know, whether the degenerate perturbation works depends on the non-diagonal term $\langle \Psi_{AKLT\parallel}^a | H | \Psi_{AKLT\parallel}^b \rangle$ vanishing or not. For an $N \times N$ square lattice model with periodical boundary condition, the wavefunction corresponding to Fig. 2(a) can be represented as

$$\Psi_{AKLT\parallel}^a = \Psi_{AKLT\parallel}^{a_1} \otimes \Psi_{AKLT\parallel}^{a_2} \cdots \otimes \Psi_{AKLT\parallel}^{a_N}, \quad (8)$$

with $\Psi_{AKLT\parallel}^{a_n}$ denoting the wavefunction of the n -th periodical 1D AKLT chain. We estimate $\langle \Psi_{AKLT\parallel}^a | H | \Psi_{AKLT\parallel}^b \rangle \sim N^2 2^{-N^2}$, which decreases extremely rapidly when N increases. So we can safely draw the conclusion that in the thermodynamic limit, the non-diagonal term is zero and the degenerate perturbation and non-degenerate perturbation give the same result.

IV. EXCITATION

We can also get some results of the low energy excitation based on our trial ground state wave function. Taken the $\Psi_{AKLT\parallel}^a$ for example, the basic picture of the low energy excitation is illustrated by Fig.3 where a singlet in an AKLT chain is excited to a triplet and propagates along the chain. Now we calculate some quantitative results of this picture using a variational technique. Since our trial ground state wave function could be written as the production of many parallel 1D AKLT chains and the correlation function between different AKLT chains is zero, the low energy excitation is similar to the 1D case^{11,19}. To find the variational wave function of the low energy excitation, we use the matrix product state.²⁰ At

a site n , we define the matrix

$$M_n = \begin{pmatrix} \sqrt{1/3} |0\rangle_n & \sqrt{2/3} | -1 \rangle_n \\ -\sqrt{2/3} |1\rangle_n & -\sqrt{1/3} |0\rangle_n \end{pmatrix}. \quad (9)$$

In terms of the matrix product, the ground state of the i -th AKLT chain could be represented as

$$|\Psi_{AKLT\parallel}^{a_i}\rangle = \prod_{n=1}^N M_n^i. \quad (10)$$

and the overall ground state is given by Eq.(8).

The excited state as shown in Fig.3(a) could be represented as

$$\Phi_{AKLT\parallel}^a(\mathbf{n}) = \Psi_{AKLT\parallel}^{a_1} \otimes \dots \Phi_{AKLT\parallel}^{a_i}(n) \dots \otimes \Psi_{AKLT\parallel}^{a_N} \quad (11)$$

where $\Phi_{AKLT\parallel}^{a_i}(n)$ denotes the state with the n -th singlet of the i -th AKLT chain being excited to a triplet. For brevity, we write $|\Phi_{AKLT\parallel}^{a_i}(n)\rangle$ as $|n\rangle$ which can be represented in terms of the matrix product as

$$|n\rangle = \prod_{m=1}^n M_m \otimes \begin{pmatrix} \sqrt{1/3} |0\rangle_{n+1} & \sqrt{2/3} | -1 \rangle_{n+1} \\ \sqrt{2/3} |1\rangle_{n+1} & \sqrt{1/3} |0\rangle_{n+1} \end{pmatrix} \otimes \prod_{m=n+2}^N M_m. \quad (12)$$

This is a state with $S_{tot}^z = 0$. After some algebra, we find that

$$\langle m | n \rangle = \delta_{m,n} + \frac{1}{9}(\delta_{m,n-1} + \delta_{m,n+1}) \quad (13)$$

$$\langle m | H | n \rangle = \frac{8J_1}{9}\delta_{m,n} - \frac{J_1}{9}(\delta_{m,n-1} + \delta_{m,n+1}) \quad (14)$$

where H is the Hamiltonian (4) or (1) with $J_1 = 2J_2$. A momentum eigenstate is thus defined as

$$|\mathbf{k}\rangle = \sum_{\mathbf{n}} e^{i\mathbf{k}\cdot\mathbf{n}} |\Phi_{AKLT\parallel}^a(\mathbf{n})\rangle, \quad (15)$$

which satisfies

$$\langle \mathbf{k} | \mathbf{k} \rangle = (1 + \frac{2}{9} \cos k_x) N^2, \quad (16)$$

$$\langle \mathbf{k} | H | \mathbf{k} \rangle = (\frac{8}{9} - \frac{2}{9} \cos k_x) N^2 J_1. \quad (17)$$

So the variational energy is

$$E_{var}(\mathbf{k}) = \frac{8 - 2 \cos k_x}{9 + 2 \cos k_x} J_1, \quad (18)$$

where we have made an energy shift of $-\frac{8}{3} J_2 N^2$ in the above calculation.

V. DISCUSSION AND GENERALIZATION

The string order was first observed in the spin-1 AKLT chain¹³. It is believed that even when the Hamiltonian deviates from the exact AKLT point, the string order did not vanish²¹. However, the nonzero string correlator was rarely observed in the 2D model, the only exception that we have known up to now is the Wen-Kitaev Model²², which is a 2D exactly solvable model with a string correlator attaining finite value. In our trial ground state, since there is a strong evidence that the 2D ground state is decoupled into several 1D AKLT chains, the order parameter¹³ proposed to characterize the 1D VBS state should also be valid in our 2D problem. We believe that the string order parameter:

$$\mathcal{O}_{string}^{\alpha} = - \lim_{|k-l| \rightarrow \infty} \langle \Psi_0 | S_{ik}^{\alpha} \exp[i\pi \sum_{j=k+1}^{l-1} S_{ij}^{\alpha}] S_{il}^{\alpha} | \Psi_0 \rangle \quad (19)$$

should get its maximum in the point $J_2/J_1=1/2$, which is still to be verified by numerical methods.

Now we discuss the case when the coupling coefficient J_2/J_1 deviates from 1/2. For the general $J_1 - J_2$ model, the RG analysis based on the nonlinear σ model can show that $J_2/J_1 = 1/2$ represents a stable fixed point in RG flow in the parameter space³, so we believe that our trial ground states represent a universal class and capture the basic property of the spin disordered phase of the spin-1 $J_1 - J_2$ model.

VI. CONCLUSION

Based on a solvable spin-1 model with dimer-type and valence-bond-solid-type ground states, we studied the fully frustrated spin-1 $J_1 - J_2$ model and proposed a possible trial ground state at the point $J_2/J_1 = 0.5$, which has been seldom studied before. Such ground states are doubly degenerate and approximately described by the decoupled AKLT states along the horizontal or vertical direction of the square lattice. We believe that this trial state captures the main character of the disordered phase in the 2D spin-1 frustrated system, and can be detected by numerical methods. In addition, the pseudo-potential method used here is not only restricted to square lattice and the spin-1 case, but also to higher spin or other lattice cases as long as the Hamiltonian could be expanded to the summation of projection operators. Taking the spin-1 Honeycomb lattice for an instance, the state with $S_{\alpha}^{total} \leq 2$ for each hexagon is close to the real ground state of the $J_1 - J_2 - J_3$ model in the Honeycomb lattice, even closer than the case of the square lattice because the perturbation takes a smaller portion in this Hamiltonian

than that in the square lattice $J_1 - J_2$ model. So our method offers a potential framework to explore quantum exotic state in spin systems.

This work is supported in part by NSF of China under Grant No. 10574150 and programs of Chinese Academy of Sciences.

APPENDIX A

In this appendix, we will prove the fact that the average value of $\mathbf{S}_i \cdot \mathbf{S}_{i+1}$ is lower in a AKLT chain with infinite length than that in a closed AKLT loop with finite length. Our proof is based on some results in Ref¹².

Let (+), (0), and (-) denote the orthonormal basis for spin 1 consisting of eigenstates of S^z with eigenvalues +1, 0, and -1, respectively and

$$\psi_{11} = \sqrt{2}(+), \quad \psi_{12} = \psi_{21} = (0), \quad \psi_{22} = \sqrt{2}(-). \quad (A1)$$

We denote the wavefunction of a single AKLT chain with length L as

$$\Omega_{\alpha\beta} = \psi_{\alpha\beta_1} \bigotimes \psi_{\alpha_2\beta_2} \cdots \psi_{\alpha_L\beta_L} \varepsilon^{\beta_1\alpha_2} \varepsilon^{\beta_2\alpha_3} \cdots \varepsilon^{\beta_{L-1}\alpha_L}, \quad (A2)$$

where $\varepsilon^{\alpha\beta}$ is the antisymmetric tensor with $\varepsilon^{12} = 1$. As shown in¹², the inner product of two AKLT chains with L sites is

$$\Omega_{\beta}^{\dagger\alpha} \cdot \Omega_{\gamma}^{\delta} = \delta_{\gamma}^{\alpha} \delta_{\delta}^{\beta} (3^L - 1)/2 + \delta_{\beta}^{\alpha} \delta_{\gamma}^{\delta}, \quad (A3)$$

so the normalization of the ground state with periodic boundary conditions reads

$$\Omega_{\beta}^{\dagger\beta} \cdot \Omega_{\alpha}^{\alpha} = 3^L + 3 \quad (A4)$$

Next we calculate the spin-spin correlation function between the site 1 and 2 $\langle S_1^z S_2^z \rangle$ for a chain with L sites and periodic boundary conditions. Following¹², the spin operators acting on our basis for a single spin 1 give rise to

$$S_1^z \psi_{\alpha\beta_1} = (1/2)[(-1)^{\alpha} + (-1)^{\beta_1}] \psi_{\alpha\beta_1}, \quad (A5)$$

$$S_2^z \psi_{\alpha_2\beta_2} = (-1/2)[(-1)^{\alpha_2} + (-1)^{\beta_2}] \psi_{\alpha_2\beta_2}. \quad (A6)$$

Combining A(2) – A(6), we can find

$$\langle S_1^z S_2^z \rangle = -4(3^{L-2} - 1)/(3^L + 3). \quad (A7)$$

We notice that the AKLT chain is isotropic, so $\langle \mathbf{S}_1 \cdot \mathbf{S}_2 \rangle = 3 \langle S_1^z S_2^z \rangle = -12(3^{L-2} - 1)/(3^L + 3)$. Now we have proven the fact that the average value of $\mathbf{S}_i \cdot \mathbf{S}_{i+1}$ is lower in an AKLT chain with infinite length than that in a closed AKLT loop with finite length. When $L \rightarrow \infty$, we get the value in¹² that $\langle \mathbf{S}_i \cdot \mathbf{S}_{i+1} \rangle = -4/3$.

^{*} Electronic address: schen@aphy.iphy.ac.cn

¹ G. Misguish and C. Lhuillier, Review article in the book

“Frustrated spin systems”, edited by H. T. Diep, World Scientific, Singapore (2005), and references therein.

² P. Chandra and B. Doucot, Phys. Rev. B **38**, 9335 (1988).

³ T. Einarsson and H. Johannesson, Phys. Rev. B **43**, 5867 (1991).

⁴ E. Fradkin, *Field theories of condensed matter systems*. (Addison-Wesley Publishing company,1991)

⁵ L. Capriotti and S. Sorella, Phys. Rev. Lett. **84**, 3173 (2000).

⁶ N. Read and S. Sachdev, Phys. Rev. B **42**, 4568 (1990); Phys. Rev. Lett. **66**, 1773 (1991).

⁷ L. Capriotti, F. Becca, A. Parola, and S. Sorella, Phys. Rev.Lett. **87**, 097201 (2001); Phys. Rev. B **67**, 212402 (2003).

⁸ O. P. Sushkov, J. Oitmaa, and Z. Weihong, Phys. Rev. B **63**, 104420 (2001).

⁹ J. J. Garcia-Ripoll, M. A. Martin-Belgado, and J. I. Cirac, Phys. Rev. Lett. **93**, 250405 (2004).

¹⁰ F. D. M. Haldane, Phys. Rev. Lett. **61**, 1029 (1988).

¹¹ D. P. Arovas, A. Auerbach, and F. D. M. Haldane, Phys. Rev. Lett. **60**, 531 (1988).

¹² I. Affleck, T. Kennedy, E. H. Lieb, and H. Tasaki, Phys. Rev. Lett. **59**, 799 (1987); Commun. Math. Phys. **115**, 477 (1988).

¹³ M. den Nijs and K. Rommelse, Phys. Rev. B **40**, 4709 (1989)

¹⁴ F. D. M. Haldane, Phys. Rev. Lett. **51**, 605 (1983).

¹⁵ C. D. Batista and S. A. Trugman, Phys. Rev. Lett. **93**, 217202 (2004).

¹⁶ C. K. Majumdar and D. K. Ghosh, J. Math. Phys. **10**, 1388(1969); B. S. Shastry and B. Sutherland, Physica B **108**, 1069 (1981).

¹⁷ S. Chen, H. Buttner and J. Voit, Phys. Rev. B **67**, 054412, (2003); Phys. Rev. Lett. **87**, 087205, (2001); S. Chen and B. Han, Eur. Phys. J. B **31**, 63, (2003).

¹⁸ Z. Nussinov and A. Rosengren, cond-mat/0504650.

¹⁹ D. Sen and N. Surendran, Phys. Rev. B **75**, 104411 (2007).

²⁰ A. Klumper, A. Schadschneider, and J. Zittartz, J. Phys. A **24**, L955 (1991).

²¹ H. Tasaki, Phys. Rev. Lett **66**, 798 (1991).

²² X.-G. Wen, Phys.Rev. Lett **90**, 016803 (2003).